Improved protection system for phase faults on marine vessels based on ratio between negative-sequence and positive-sequence of the fault current

Catalin Iosif Ciontea [1*], Qiteng Hong [2], Campbell Booth [3], Claus Leth Bak [4], Frede Blaabjerg [5], Kjeld Kilsgaard Madsen [6], Claes Høll Sterregaard [7]

[1, 4, 5] Department of Energy Technology, Aalborg University, Pontoppidanstraede 111, 9220 Aalborg East, Denmark
[2, 3] Department of Electronic and Electrical Engineering, University of Strathclyde, George Street 204, G1 1XW Glasgow, United Kingdom
[1, 6, 7] Department of Research and Development, DEIF A/S, Frisenborgvej 33, 7800 Skive, Denmark
[*]cic@deif.com

Abstract: This paper presents a new method to protect the radial feeders on marine vessels. The proposed protection method is effective against Phase-Phase (PP) faults and is based on evaluation of the ratio between the negative-sequence and positive-sequence of the fault currents. It is shown that the magnitude of the introduced ratio increases significantly during the PP fault, hence indicating the fault presence in an electric network. In this paper, the theoretical background of the new method of protection is firstly discussed, based on which the new protection algorithm is described afterwards. The proposed algorithm is implemented in a programmable digital relay embedded in a Hardware-in-the-Loop (HIL) test setup that emulates a typical maritime feeder using a Real Time Digital Simulator (RTDS). The HIL setup allows testing of the new protection method under a wide range of faults and network conditions and the experimental results demonstrate its effectiveness in all scenarios conducted. The proposed protection method offers a solution to the protection challenges associated with variability of the short-circuit currents in radial feeders, advancing in this way the traditional mean of protection in maritime feeders, represented by OverCurrent (OC) relays.

1. Introduction

Vessels are used from ancient times, but only since the end of the 19th century electricity is integrated into their structure [1]. Nowadays electricity is essential for several systems on board and operation of a vessel or of another maritime application without a functional electric network is unconceivable [1], [2]. Propulsion, maneuvering, navigation, signalling, lighting, communication, ventilation, heating and cooling are just some of the shipboard systems dependent on the availability of the electric power on board [2]. Both DC and AC electric systems are used in the maritime sector, but most vessels employ an AC (at 50 Hz or 60 Hz) network [2] and therefore only the maritime AC networks are discussed in this paper.

The electric AC network of a vessel can be considered as an islanded microgrid where all electricity is generated, distributed and consumed within the limits of a reduced area, represented by the vessel itself [3]. Generation is provided by a number of generators and is variable, as the energy needs of the vessel are variable as well [4]. In general, distribution of the electric power is realised radially and involves the use of multiple voltage levels [3]. The nominal voltage ranges from the typical household voltage level (e.g. 110 V or 230 V) to several kilovolts, with the maximum allowed voltage limited to 15 kV in most vessels [5]-[7]. The network is typically ungrounded below 1 kV and grounded via a high impedance above 1 kV [8], [9]. With these grounding arrangements, Phase-to-Ground (PG) faults do not produce significant fault currents. Consequently the electric network of a vessel allows continuity of supply in the event of a single PG fault, which is the most common electric fault that occurs in maritime applications [10].

Protection against the electric faults is of paramount importance on vessels, as the loss of any system on board could result in dangerous conditions for the vessel or for personnel safety [3]. The damage produced by a short-circuit is proportional with the fault current [11] and on vessels PP and Three-Phase (3P) faults produce the most intense fault currents. OC protection is widely used for detection of these abnormal conditions on vessels [1], but its correct operation can be compromised in some cases. For example, variable generation may lead to variation of the available short-circuit power, thereby endangering coordination of the OC relays [4], while the relatively reduced fault currents could cause longer tripping times for the relays [12]. Moreover, these protection problems could be more pronounced in the future, as it is anticipated that the new vessel designs will introduce more variable generation and load levels [13]. Furthermore, the resistance of the fault adds as another factor that affects the tripping times of the OC relays. Therefore, the conventional OC protection needs to be revised in maritime applications with a high degree of variability of the fault current.

In response to the protection issues caused by variable short-circuit power in maritime applications, a new method of protection has been suggested in [12] against PP faults. The method proposed in [12] uses symmetrical components of the fault currents and communication between the protection relays to clear PP faults in a maritime feeder in a selective manner. However, if communication between the protection relays is lost then coordination is no longer possible and the protection system loses selectivity. Also, the relay-dedicated communication is not always available on vessels and when it is available, a backup protection method is still needed in the event of a communication failure scenario. In this paper the protection method proposed in [12] is modified so that

communication is no longer required, thus making it suitable for a wider range of vessels. The newly developed method of protection addresses PP faults because 3P faults are very rare on vessels and usually develop from PP faults [13], while PG faults do not produce significant fault currents on vessels, as discussed previously.

The protection method proposed in this paper has been implemented in a programmable digital relay and tested in a HIL setup that emulates a maritime feeder using RTDS, and the experimental results show that it provides satisfactory performance for a wide range of conditions. The conditions examined include variable levels of short-circuit power and different fault resistances.

2. Electric network of a vessel

The AC network of a vessel is characterized by a redundant design such that a single electrical fault does not cause the loss of any essential system on board [1]-[3]. The redundant design is achieved by duplication of the electric equipment in a way that most of the loads can be powered using at least two independent electric paths and by physical separation of the duplicated equipment so that a single defect cannot affect them simultaneously [1], [2]. In fault conditions the electric network is reconfigured using various Circuit Breakers (CBs) and the electric energy is transmitted to the loads using a healthy path, but the radial structure of the network is preserved [3]. This concept is illustrated in Fig. 1, where a typical AC network on a vessel is devised.

In healthy conditions, all CBs are closed, with the exception of CB_{34} and CB_{56}, which are kept open. The network can be split in two radial paths: Bus 1 - Bus 3 - Bus 5 and Bus 2 - Bus 4 - Bus 6. In the event of a fault, e.g. on *Tr.1*, CB_{13} and CB_{31} will be opened and CB_{34} will be closed, so all loads continue to be fed, while the radial structure of the network is preserved. The same logic is used even if the electric fault occurs in other locations and reconfiguration of the network ensures that the supply of most consumers is maintained during the fault conditions. The protection of the electric network shown in Fig. 1 is reduced to the protection of the two radial paths mentioned before and their associated electric equipment.

3. Proposed protection method

3.1. The method of symmetrical components

The method of symmetrical components represents a practical engineering tool for analysis of the electric circuits under unbalanced conditions. The symmetrical components

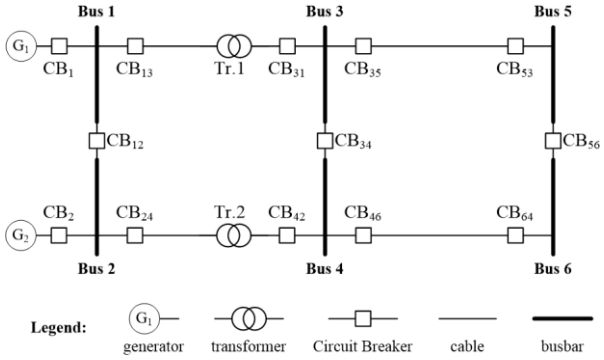

Fig. 1 *Typical AC network of a vessel*

of a set of three phasors consist from the followings: the positive-sequence quantities (PSQ), the negative-sequence quantities (NSQ) and the zero-sequence quantities (ZSQ). In general, three-phase generators are designed to produce only PSQ, while NSQ and ZSQ are produced by asymmetries of the electric network [15]. More precisely, NSQ are produced by any imbalance that occurs in the network and ZSQ are produced by any imbalance that involves the ground [16].

Compared to the phase-quantities of the voltage and current, their sequence-components counterparts are more sensitive to asymmetric faults [16], hence many protection relays rely on these quantities [15]. For example, all ground relays operate on ZSQ [15], differential protection can be stabilized using NSQ [17] and directional elements can be polarized by NSQ and ZSQ [16]. In this paper, symmetrical components have been used for analysis of a radial feeder during PP faults and based on this analysis, a new method of protection for these faults has been developed.

3.2. Analysis of a radial feeder during the PP fault

Analysis of a radial feeder during the PP fault is realised using the network shown in Fig. 2a, resembling a maritime radial feeder. It consists of a three-phase power source grounded through a resistance R_G and three balanced delta loads. Monitoring of the feeder currents is realised for protection purposes by three sets of Current Transformers (CTs), denoted as *CT1*, *CT2* and *CT3*. The currents seen by the CTs are labelled I_{CT1}, I_{CT2} and I_{CT3}, while the load currents are denoted I_{L1}, I_{L2} and I_{L3}. A PP fault with a resistance R_F is applied on feeder as indicated in Fig. 2a and the fault current is seen by *CT1* and *CT2*, while *CT3* is located downstream the fault. Analysis of the described feeder seeks to determine PSQ and NSQ of the currents seen by the indicated CTs, as only these currents are available for protection, while ZSQ are not involved in PP faults.

The pursued currents are determined by solving of the feeder sequence impedance diagram, shown in Fig. 2b, where the following notations are used. I_{1_F} and I_{2_F} are the PSQ and

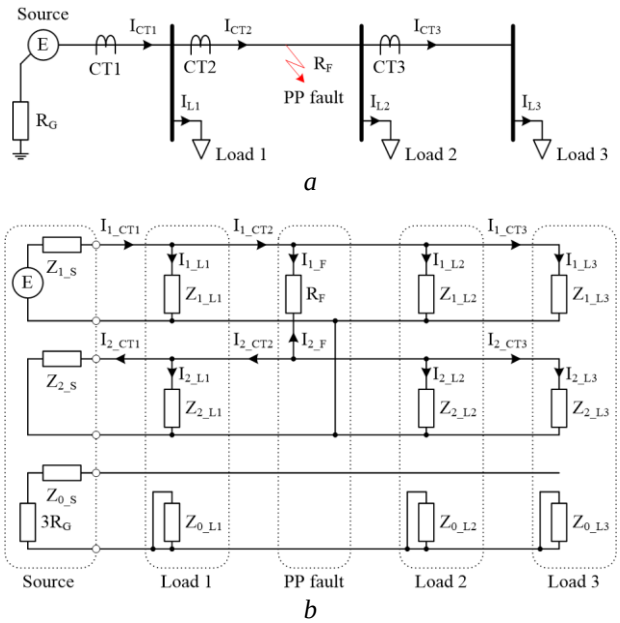

Fig. 2 *Radial feeder in PP fault conditions*
(a) *three-phase diagram,* ***(b)*** *sequence impedance diagram*

NSQ respectively of the fault current. Z_{1_S}, Z_{2_S} and Z_{0_S} are the sequence impedances of the source. Z_{1_Lx}, Z_{2_Lx} and Z_{0_Lx} are the sequence impedances of the loads. I_{1_Lx} and I_{2_Lx} are the PSQ and NSQ respectively of the load currents. I_{1_CTx} and I_{2_CTx} are the PSQ and NSQ respectively of the currents seen by the CTs. As appropriate, x is either the load indicator or the CT indicator.

I_{1_CT1} is obtained in relation (1), where Z_2 represents the equivalent negative-sequence impedance of the studied feeder and is given in (2).

$$I_{1\_CT1} = \frac{E}{Z_{1\_S} + Z_{1\_L1} \,P\, Z_{1\_L2} \,P\, Z_{1\_L3} \,P\, (R_F + Z_2)} \tag{1}$$

$$Z_2 = Z_{2\_S} \,P\, Z_{2\_L1} \,P\, Z_{2\_L2} \,P\, Z_{2\_L3} \tag{2}$$

I_{1_L1} and I_{1_CT2} are expressed as a function of I_{1_CT1} and are given in (3) and (4).

$$I_{1\_L1} = \frac{Z_{1\_L2} \,P\, Z_{1\_L3} \,P\, (R_F + Z_2)}{Z_{1\_L1} + Z_{1\_L2} \,P\, Z_{1\_L3} \,P\, (R_F + Z_2)} \cdot I_{1\_CT1} \tag{3}$$

$$I_{1\_CT2} = \frac{Z_{1\_L1}}{Z_{1\_L1} + Z_{1\_L2} \,P\, Z_{1\_L3} \,P\, (R_F + Z_2)} \cdot I_{1\_CT1} \tag{4}$$

I_{1_F} and I_{1_L2}+I_{1_CT3} are calculated based on I_{1_CT2} in (5) and (6) respectively. I_{2_F} has the same amplitude, but opposite sign compared to I_{1_F} and is given in (7).

$$I_{1\_F} = \frac{Z_{1\_L2} \,P\, Z_{1\_L3}}{R_F + Z_2 + Z_{1\_L2} \,P\, Z_{1\_L3}} \cdot I_{1\_CT2} \tag{5}$$

$$I_{1\_L2} + I_{1\_CT3} = \frac{R_F + Z_2}{R_F + Z_2 + Z_{1\_L2} \,P\, Z_{1\_L3}} \cdot I_{1\_CT2} \tag{6}$$

$$I_{2\_F} = -\frac{Z_{1\_L2} \,P\, Z_{1\_L3}}{R_F + Z_2 + Z_{1\_L2} \,P\, Z_{1\_L3}} \cdot I_{1\_CT2} \tag{7}$$

I_{2_CT2} and I_{2_L2}+I_{2_CT3} are calculated as a function of I_{1_F} and are given in (8) and (9). Furthermore, I_{2_CT1} is obtained in (10) as a function of I_{2_CT2}.

$$I_{2\_CT2} = \frac{Z_{2\_L2} \,P\, Z_{2\_L3}}{Z_{2\_S} \,P\, Z_{2\_L1} + Z_{2\_L2} \,P\, Z_{2\_L3}} \cdot I_{1\_F} \tag{8}$$

$$I_{2\_L2} + I_{2\_CT3} = \frac{Z_{2\_S} \,P\, Z_{2\_L1}}{Z_{2\_S} \,P\, Z_{2\_L1} + Z_{2\_L2} \,P\, Z_{2\_L3}} \cdot I_{1\_F} \tag{9}$$

$$I_{2\_CT1} = \frac{Z_{2\_L1}}{Z_{2\_S} + Z_{2\_L1}} \cdot I_{2\_CT2} \tag{10}$$

Finally, I_{1_CT3} and I_{2_CT3} are given in (11) and (12) as a function of I_{1_L2}+I_{1_CT3} and I_{2_L2}+I_{2_CT3} respectively.

$$I_{1\_CT3} = I_{1\_L3} = \frac{Z_{1\_L2}}{Z_{1\_L2} + Z_{1\_L3}} \cdot (I_{1\_L2} + I_{1\_CT3}) \tag{11}$$

$$I_{2\_CT3} = I_{2\_L3} = \frac{Z_{2\_L2}}{Z_{2\_L2} + Z_{2\_L3}} \cdot (I_{2\_L2} + I_{2\_CT3}) \tag{12}$$

I_{2_CT1}, I_{2_CT2} and I_{2_CT3} are indicators of the PP fault, since their magnitude is 0 only in healthy conditions, where R_F=∞. However, instead of using directly these quantities to detect the PP fault, the ratio between the current NSQ and current PSQ is suggested as a fault indicator, and the reason of this choice is given in the following section.

3.3. Ratio between current NSQ and current PSQ

The ratio between the NSQ and PSQ of the currents seen by *CT1*, *CT2* and *CT3* are calculated in (13) - (15).

$$\frac{I_{2\_CT1}}{I_{1\_CT1}} = \frac{I_{2\_CT2}}{I_{1\_CT2}} \cdot \frac{Z_{2\_L1}}{Z_{2\_S} + Z_{2\_L1}} \cdot \frac{Z_{1\_L1}}{Z_{1\_L1} + Z_{1\_L2} \,P\, Z_{1\_L3} \,P\, (R_F + Z_2)} \tag{13}$$

$$\frac{I_{2\_CT2}}{I_{1\_CT2}} = -\frac{Z_{2\_L2} \,P\, Z_{2\_L3}}{Z_{2\_S} \,P\, Z_{2\_L1} + Z_{2\_L2} \,P\, Z_{2\_L3}} \cdot \frac{Z_{1\_L2} \,P\, Z_{1\_L3}}{R_F + Z_2 + Z_{1\_L2} \,P\, Z_{1\_L3}} \tag{14}$$

$$\frac{I_{2\_CT3}}{I_{1\_CT3}} = \frac{Z_2}{R_F + Z_2} \cdot \frac{Z_{1\_L3}}{Z_{2\_L3}} \tag{15}$$

The introduced ratios are complex numbers and can be calculated with ease by a modern digital relay and used in protection. The minus sign in (14) is due to the fact that I_{1_CT2} and I_{2_CT2} flow on opposite directions. Indeed, I_{1_CT2} flows out of the source, while I_{2_CT2} flows into the source, as can be seen in Fig. 2b. Similarly, I_{1_CT1} and I_{2_CT1} are characterized by an opposite direction of flow. Contrairiwise, I_{1_CT3} and I_{2_CT3} are flowing in the same direction, to *Load 3*.

In the absence of the PP fault, the magnitude of the introduced ratios is 0, but during the PP fault their magnitude increases significantly. However, unlike the NSQ currents, whose magnitudes can take any value, relationships (13) and (14) reveal that the magnitude of the ratios seen by the CTs located upstream the PP fault, namely *CT1* and *CT2*, cannot exceed 1. Still, the magnitude of ratio seen by *CT3*, which is located downstream the PP fault, is not limited to 1, but it depends on the equivalent sequence impedances of *Load 3*, as shown by relation (15).

Relation (13) reveals that the magnitude of the ratio seen by *CT2* is greater than one seen by *CT1* as long as Z_{1_L1} and Z_{2_L1} are finite. In other words, in a radial feeder, the nearest upstream CT to a PP fault will depict the highest magnitude of the ratio between the current NSQ and current PSQ. Precisely this information is used in [12] to achieve coordination of those protection relays that rely on the ratio between the current NSQ and current PSQ. However, such coordination is not possible without communication between

the protection relays and consequently a new method of relay coordination that does not require communication is proposed in the following section.

3.4. Relay coordination without communication

The presence of PP faults in a radial feeder is indicated by a non-zero magnitude of the ratio between the current NSQ and current PSQ for all CTs on the feeder. However, this ratio is different than zero even in the absence of the PP fault in the event of some network unbalances, caused by generation or by the loads. As a result, the relay should trip only if the ratio between the current NSQ and current PSQ exceeds a pre-set threshold. Moreover, only those relays placed upstream the fault location should trip, therefore an additional criteria is used to generate the trip signal. The criteria is that a relay trips only if the current magnitude at its own location exceeds a pre-set threshold, set slightly higher than the rated current of the feeder on that location. In a radial feeder, only the relays placed upstream the fault fulfil this criteria, while the relays placed downstream the fault do not meet it. In this way, even though the rated current of a feeder can be exceeded when an electric load is turned on, this criteria alone is not sufficient for a relay to trip. Additionally, the relay should not trip if the magnitude of the ratio between the current NSQ and current PSQ exceeds 1 because this condition is possible only for a relay placed downstream the fault location, which should not trip anyway in this case.

Finally, the authors propose utilisation of a definite time-delay for each relay in order to achieve coordination of all relays in the feeder, i.e. when the PP fault is detected, a relay waits for a pre-defined time-delay before it trips and this delay is selected in such a way that clearance of the fault is realised selectively. In a radial feeder, the definite time-delay should be made longer if a relay is closer to the generators, while the relay located at the end of the feeder should trip after the shortest delay.

Fig. 3 presents the logical structure of the discussed protection algorithm for a single relay, where the following notations are used: $I_{threshold}$ is the current that needs to be exceeded at the location of the relay, $I_2/I_{1\_threshold}$ is the pre-set threshold that needs to be exceeded by the magnitude of the proposed ratio during PP faults and t_{delay} is the pre-set definite time-delay after which the relay trips.

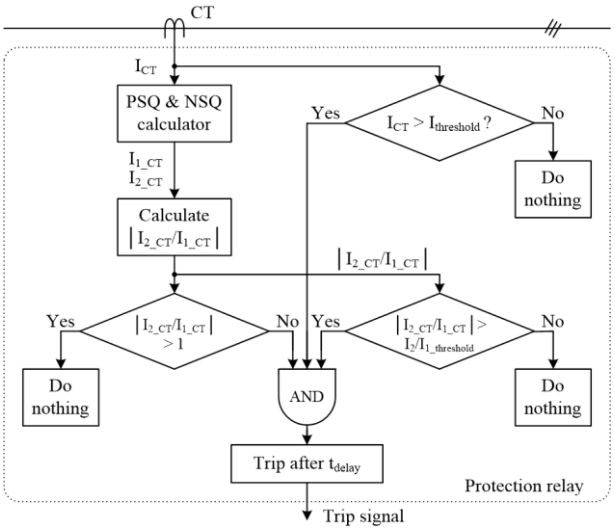

Fig. 3 *Logical algorithm of the proposed relay*

4. Experimental setup

The proposed method of protection has been tested using the HIL setup shown in Fig. 4a. The HIL setup consists from an RTDS, a signal amplifier and a programmable digital relay. RTDS emulates the maritime radial feeder shown in Fig. 4b and outputs a three-phase AC signal proportional with the three-phase current seen by one of the CTs indicated in Fig. 4b. The AC signal is amplified afterwards by the signal amplifier and injected into the digital relay. Through the "Selector" block, selection of the appropiate signal allows for the digital relay to be connected to any of the available CTs in the feeder emulated on RTDS. The purpose of the signal amplifier is to ensure the interface between RTDS and the digital relay used in this setup, as RTDS outputs a 10 V AC signal, while the relay requires a 10 A AC input.

The maritime feeder shown in Fig. 4b is powered by two synchronous generators: a 7.2 MVA generator, denoted as G_1 and a 4.8 MVA generator, denoted as G_2. The feeder consists of five electric loads placed on five bus bars that are interconnected by five cables, labelled L_{xy}, where x and y are indicators of the adjacent bus bars. The loads are balanced, which is typical in a MV feeder on a vessel. Also, a 2 MVA transformer, denoted *Tr.*, exists between between cable L_{23} and *Bus 3*. Implementation of the described feeder on RTDS is realised using the standard models available in RSCAD for generators, transformer and loads, while the electric cables are modelled using a π-model. The main parameters of the generators, transformer, loads and cables are given in [12].

The relay used in the HIL setup is manufactured by DEIF A/S [18] and is modified in order to accommodate the protectection algorithm described in the previous section of the paper. The internal parameters of the relay and the fault record are accesible to a user and can be downloaded on a computer. In this way, the ratio between the current NSQ and current ZSQ, and the three-phase currents, as calculated by the digital relay are examined for various faults and network conditions in order to evaluate the fesability of the proposed method of protection.

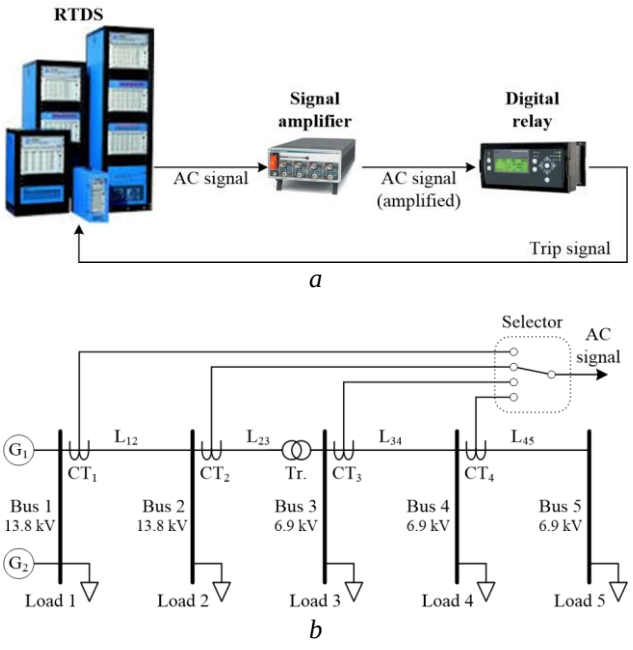

Fig. 4 *Experimental setup*
(a) *HIL setup diagram,* ***(b)*** *maritime feeder on RTDS*

The digital relay is connected alternatively at each set of CTs of the feeder shown in Fig. 4b and the relay is set according to the location selected. The protection settings of the relay for each CT are given in Table 1. A PP fault is applied between *phase b* and *phase c* at various locations on the feeder. When applied on a cable, the fault appears in the middle of it. For each fault, the conditions of the network are modified in order to emulate variable generation and various fault resistances. Generation is varied by turning on or off a generator and affects the available short-circuit power on the feeder. The following fault resistances are considered: 0 Ω to emulate a bolted fault, 2 Ω to emulate a typical arcing fault occurring in a network operating at similar voltage levels as the test maritime feeder [19] and 10 Ω to emulate a fault with a higher resistance. The most interesting results are discussed in followings.

5. Experimental results

5.1. Fault occurring downstream the relay

Fig. 5a presents the three-phase currents and the ratio between the current NSQ and current PSQ, as calculated by the digital relay when connected to CT2 for a bolted PP fault occurring on cable L_{23} in the event that the electric network is powered by G_2. During the fault, the phase current exceeds $I_{threshold}$ (set to 111 A in this case), while the ratio between the current NSQ and current PSQ exceeds $I_2/I_{1\_threshold}$ (set to 0.2), but without surpassing 1. As a result, the digital relay detects correctly the presence of the PP fault downstream to its own location and clears the fault after a delay of 600 ms, in accordance with the relay settings shown in Table 1. The magnitude of the ratio between the current NSQ and current PSQ does not vary too much during the fault and it takes 1-2 periods of time after the fault inception before it exceeds the pre-set threshold. This delay is caused by internal calculations of the digital relay.

Table 1 Settings of the digital relay according to CT location

Relay location	$I_2/I_{1\_threshold}$	$I_{threshold}$ [A]	t_{delay} [ms]
CT1	0.2	217	800
CT2	0.2	111	600
CT3	0.2	126	400
CT4	0.2	55	200

Fig. 5b presents the three-phase current and the ratio between the current NSQ and current PSQ, as calculated by the digital relay when connected to CT2 for a bolted PP fault occurring on *Bus 3* for the same conditions as considered before. The fault is detected by the relay in a similar manner as in the previous case. Even though the phase currents are greatly reduced for a PP fault occurring on *Bus 3*, compared to a PP fault occurring on cable L_{23}, the magnitude of the ratio between the NSQ and PSQ of the measured current is only marginally smaller. The PP fault is cleared after a delay of 600 ms, in accordance with the protection settings given in Table 1. In other words, the ratio is not affected significantly by variability of the short-circuit currents and the new method of protection is not endangered by this condition.

The PP faults applied on cable L_{23} or *Bus 3* should not be detected only by a relay connected on CT2, but also by a relay connected to CT1. Moreover, the latter provides backup protection for the relay connected on CT2. In order to test such scenario, the same PP fault and network conditions as considered in Fig. 5a and Fig. 5b are considered again, but this time the digital relay is connected to CT1.

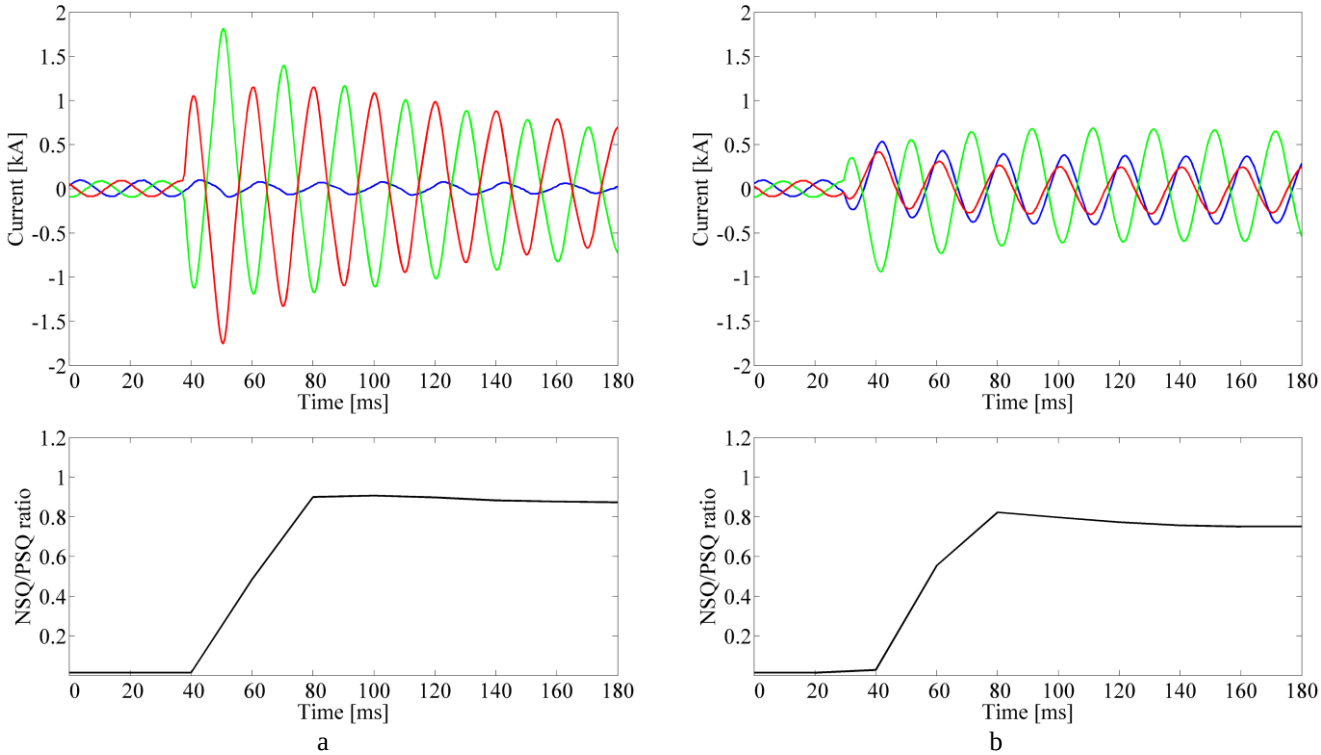

Fig. 5 *Phase currents and the ratio between current NSQ and current PSQ as seen by the digital relay connected to CT2 for a bolted fault, while the feeder is powered by G_2:* ***(a)*** *PP occurs on L_{23},* ***(b)*** *PP fault occurs on Bus 3*

Fig. 6a illustrates the phase currents and the ratio between the current NSQ and current PSQ, as calculated by the digital relay connected to CT1 for a bolted PP fault occurring on cable L_{23} with the feeder powered by G_2. The phase current exceeds $I_{threshold}$ (set to 217 A in this case) during the fault, while the ratio between the current NSQ and current PSQ exceeds $I_2/I_{1\_threshold}$ (set to 0.2), but without surpassing 1. The relay detects correctly the presence of the fault downstream to its own location and the trip signal is generated after a delay of 800 ms, in accordance with the settings given in Table 1. Consequently, the relay connected to CT2 clears the PP fault before the relay connected to CT1, hence coordination of the protection relays and the back-up functionality are both ensured.

Fig. 6b illustrates the phase currents and the ratio between the current NSQ and current PSQ, as calculated by the digital relay when connected to CT1 for a bolted PP fault occurring on *Bus 3* with the feeder powered by G_2. The PP fault is detected correctly, as the phase current, respectively the ratio between the current NSQ and current PSQ exceed their corresponding thresholds. As can be seen in Fig. 6, even though the phase currents are greatly reduced for a PP fault occurring on *Bus 3*, compared to a PP fault occurring on cable L_{23}, the magnitude of the ratio between the NSQ and PSQ of the measured current is only marginally smaller. The trip signal is generated after a delay of 800 ms, longer than the delay associated with the relay connected to CT2 and only if the PP fault persists, thus selectivity and the back-up function are both ensured.

The relay connected to CT1 notices a slightly smaller ratio between the current NSQ and current PSQ than the relay connected to CT2, as comparison between Fig. 5a and Fig. 6a, and Fig. 5b and Fig. 6b respectively reveals. The result is in accordance with the theory discussed in previous sections of the paper, thus confirming that the nearest upstream relay to a PP fault depicts the highest magnitude of the ratio between the current NSQ and current PSQ.

5.2. Fault in variable network conditions

Fig. 7a presents the ratio between current NSQ and current PSQ, as calculated by the digital relay connected alternatively to each set of CTs on the feeder for various fault conditions. The PP fault is applied on the middle of the cable where the digital relay is connected. For each fault, the ratio is presented as an interval of values instead of a single value because the ratio is not entirely constant during the fault, as the previous figures show. The mean values of each interval are connected with a line for a better visualization of the variation of the ratio in different network conditions. Also, to put things in perspective, variation of the ratio between the current NSQ and current PSQ is compared with variation of the phase currents, seen by the same relay for the same set of network conditions. Accordingly, Fig. 7b illustrates the phase currents seen by the digital relay connected alternatively to each set of CTs on the feeder for the same network conditions and PP faults as in Fig. 7a.

Fig. 7a shows that in all conditions, the magnitude of the ratio between the NSQ and PSQ of the fault current is approaching 1, but without surpassing this value. This result is in accordance with the theoretical background discussed earlier in this paper. Fig. 7a also shows that the magnitude of the ratio between current NSQ and current PSQ is decreasing with the decrease of the available short-circuit power, but its variation is not significant. Moreover, the magnitude of the ratio between the current NSQ and current PSQ is decreasing with the increase of the fault resistance as well, but even in this case its variation is not significant. In all cases considered, during the PP fault, the magnitude of the ratio between the

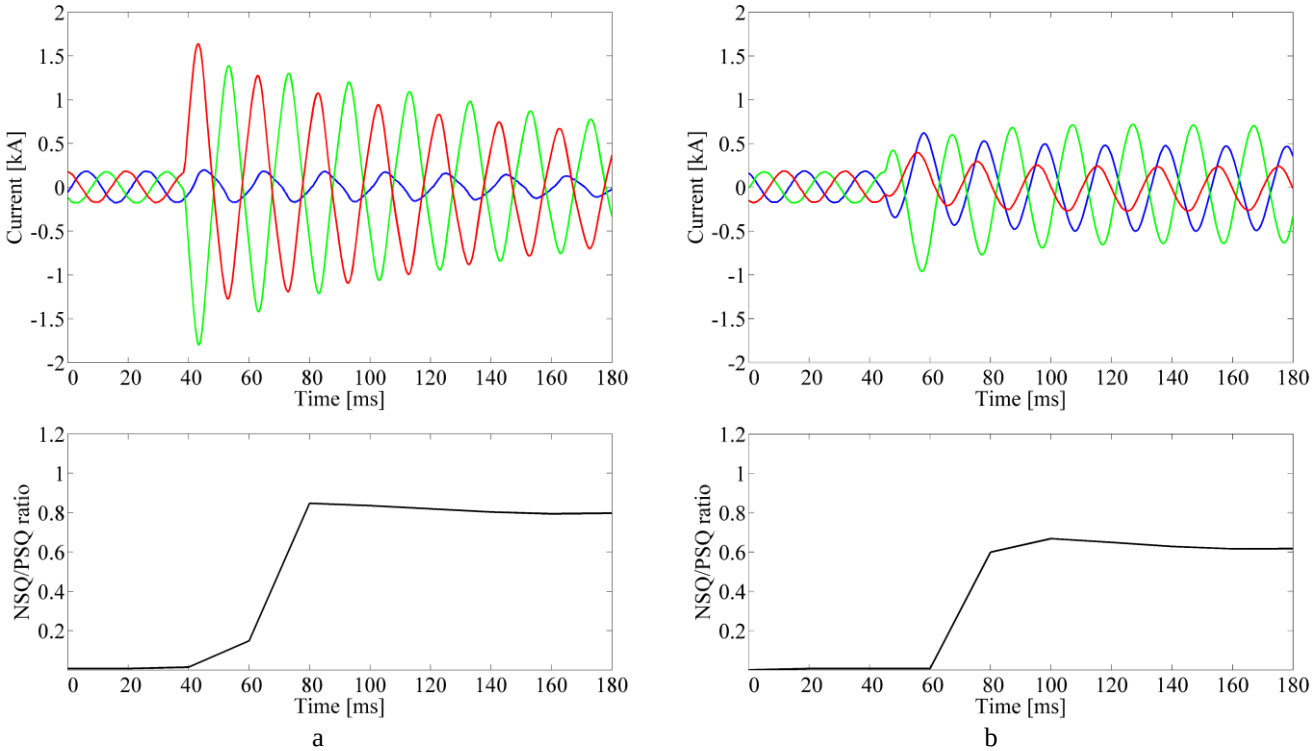

Fig. 6 *Phase currents and the ratio between current NSQ and current PSQ as seen by the digital relay connected to CT1 for a bolted fault, while the feeder is powered by G_2:* ***(a)*** *PP occurs on L_{23},* ***(b)*** *PP fault occurs on Bus 3*

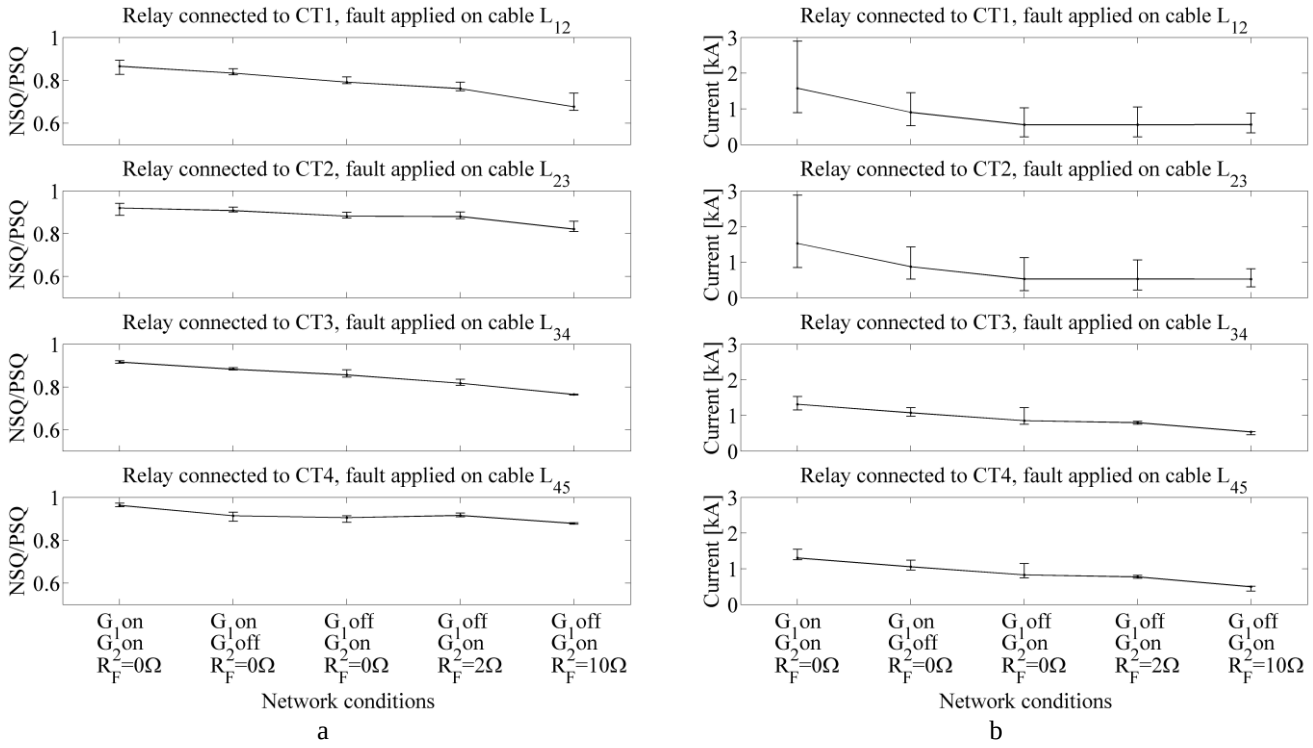

Fig. 7 *Effect of variable generation and variable fault resistance at various locations:* ***(a)*** *ratio between current NSQ and current PSQ,* ***(b)*** *phase RMS currents*

current NSQ and current PSQ is far greater than the pre-set threshold value (0.2 for all relays) and the PP fault is cleared successfully within an acceptable time frame. The minimum and maximum tripping times associated with the new method of protection for the same faults and network conditions as considered in Fig. 7 are given in Table 2.

Fig. 7b shows that the phase currents vary more than the magnitude of the ratio between current NSQ and current PSQ with variation of the network conditions. For example, the phase current seen by CT1 during the PP fault varies from about 0.3 kA to 3 kA, with the mean current varying from about 0.5 kA to 1.5 kA, while the magnitude of the ratio between the NSQ and PSQ of the current seen by the same CT varies from about 0.65 to 0.85. The same trend is valid for other CTs as well. This result suggests that if conventional OC protection is employed in this feeder, then it would be challenged by variability of the short-circuit currents. In order to test this hypothesis, the digital relay is programmed to trip using the IEC standard inverse characteristic [20]. The minimum and maximum tripping times associated with OC protection for the same PP faults and network conditions as considered in Fig. 7 are given in Table 3. The settings of OC protection are given in Table 4 and are chosen in such a way that the time margin between two consecutive locations of the relay on feeder is 200 ms, similarly as for the new protection method proposed in this paper.

Comparison between the tripping times indicated in Table 2 and Table 3 reveals the superiority of the new method of protection over OC protection in terms of tripping speed for the experimental tests performed. Variability of the fault current causes almost no difference between the minimum and maximum tripping times in case of protection based on the ratio between the current NSQ and current PSQ. On the contrary, variability of the fault current causes relatively large differences between the minimum and maximum tripping times in case of OC protection. These results also suggest that in feeders with high variability of short-circuit currents, OC relays should be adaptive to network conditions in order to avoid the unnecessary long tripping times. Contrariwise, the proposed method of protection does not need to be adaptive because a single set of settings is sufficient for a wide range of network conditions. For these reasons, the new protection method introduced in this paper advances the traditional way of protection in maritime feeders.

Table 2 Tripping times corresponding to protection based on I_2/I_1 ratio for conditions considered in Fig. 7

Relay location	Minimum tripping time [ms]	Maximum tripping time [ms]
CT1	830	835
CT2	630	639
CT3	431	437
CT4	232	240

Table 3 Tripping times corresponding to conventional OC protection for conditions considered in Fig. 7

Relay location	Minimum tripping time [ms]	Maximum tripping time [ms]
CT1	666	2284
CT2	450	1105
CT3	445	706
CT4	239	341

Table 4 Settings of OC protection according to CT location

Relay location	Time multiplier setting	Pick-up current [A]
CT1	0.20	217
CT2	0.17	111
CT3	0.14	126
CT4	0.10	55

5.3. Fault occurring upstream the relay

Another interesting scenario is represented by the case when the PP fault is applied upstream to the location of the relay. Fig. 8a presents accordingly the three-phase current and the ratio between the current NSQ and current PSQ, as calculated by the digital relay connected to CT2 for a bolted PP fault occurring on cable L_{12} in the event that the feeder is powered by G_2. In this case, even though the ratio between the current NSQ and current PSQ exceeds the pre-defined threshold, the relay does not trip because the magnitudes of the phase currents do not increase during the fault above the pre-defined threshold (set to 111 A in this case). The relay operates correctly by not tripping, as the PP fault occurs upstream the relay location and therefore it should be cleared by another relay in this case.

The same scenario is followed alternately for other conditions of the electric network. The experimental tests show that variation of the available short-circuit power does not affect the ratio seen by a relay connected to CT2 for a bolted PP fault on cable L_{12}, but the resistance of the PP fault has a pronounced effect on this ratio. For example, Fig. 8b illustrates the three-phase current and the ratio between the current NSQ and current PSQ, as calculated by the relay connected to CT2 in the event that the feeder is powered by G_2 and a PP fault with a resistance of 10 Ω is applied on cable L_{12}. Again, the relay operates correctly by not tripping, as the magnitudes of the phase currents do not increase above the pre-defined threshold. Compared to the bolted PP fault scenario, in this case the fault resistance causes a significant lower value of the magnitude of the ratio between the current NSQ and current PSQ, but without affecting the proposed protection system. However, it must be noticed that these relatively large variations of the ratio between the current NSQ and current PSQ are characteristics only for a relay located downstream the fault, while a relay located upstream the fault sees a much smaller variation of the same ratio, as shown in previous sections.

5.4. Effect of electric motors on protection

The protection system in a marine vessels must handle the Induction Motors (IMs) that are connected directly to the electric network. Such IMs are used to drive various pumps on vessels and their starting current should not cause tripping of the protection relays. Also, IMs contribute to fault currents and can cause reverse current flows. In order to test the effect of IMs on the proposed protection system, a three-phase IM with rated power of 0.5 MVA is connected on *Bus 3* and then bolted PP faults are applied alternatively at various locations on the electric network. The results of these tests demonstrate that the fault contribution of the studied IM during PP faults does not affect the performance of the proposed protection system. Moreover, similar results are obtained for other fault resistances and the starting current of the IM did not cause the mal-operation of the protection system, so it can be concluded that the protection method proposed in this paper is not affected by directly-connected IMs.

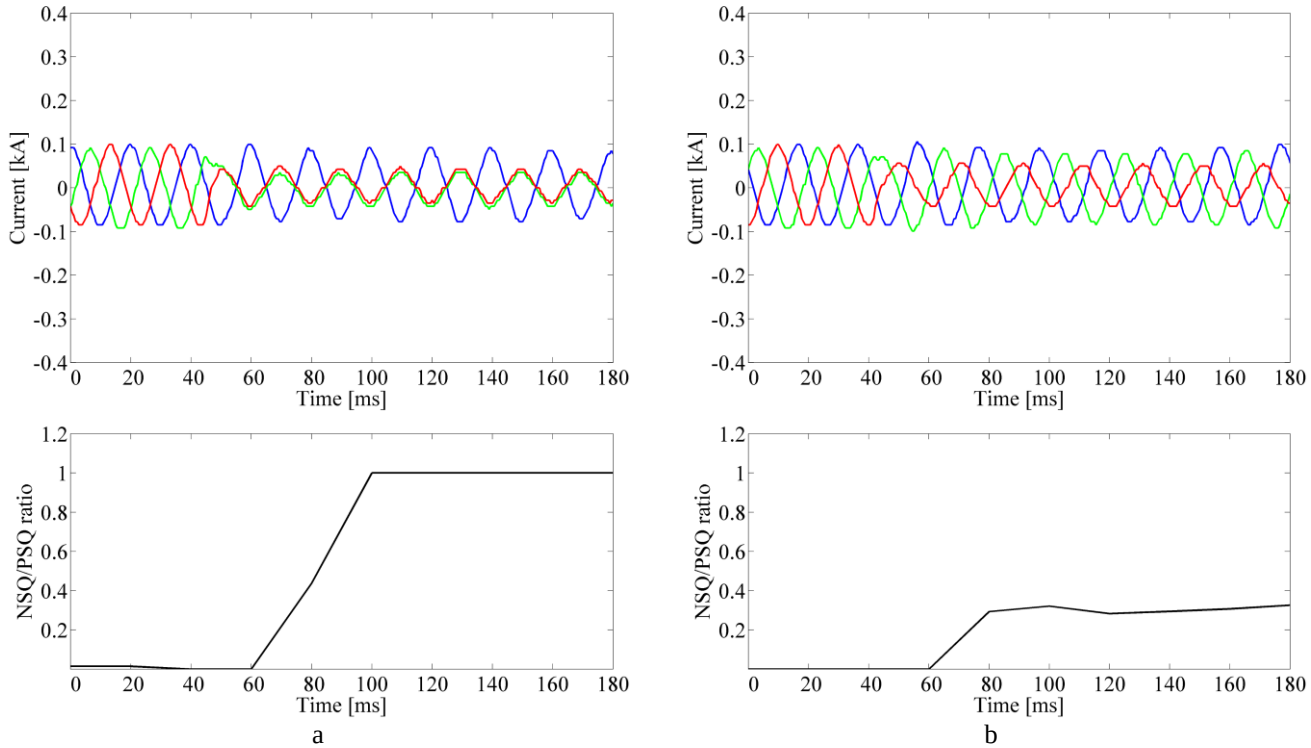

Fig. 8 *Phase currents and the ratio between current NSQ and current PSQ as seen by the relay connected to CT2 in eventuality that the feeder is powered only by G_2:* ***(a)*** *PP occurs on L_{12} (R_F = 0 Ω),* ***(b)*** *PP fault occurs on L_{12} (R_F = 10 Ω)*

6. Conclusion

The basic principles of a new protection method for PP faults in a maritime radial feeder have been presented in this paper and the proposed protection algorithm has been tested in an experimental test setup. In the proposed method, detection of PP faults is based on evaluation of the magnitude of the ratio between the current NSQ and current PSQ, which experiences a significant increase during the fault. The new protection method is implemented in a programmable digital relay and is tested in various network conditions, including variable short-circuit power and various fault resistances, using a real-time HIL testbed. The experimental results prove that operation of the tested relay, thus the proposed protection system is not affected by variable network conditions and all PP faults were detected successfully.

The advantages of the method of protection based on the ratio between the current NSQ and current PSQ include simplicity of the setting procedure, as no prior knowledge of the fault levels is required and the fact that a single set of settings is valid for a wide range of network conditions. The findings of this paper suggest that the proposed method of protection delivers significant improvement of performance over conventional OC relays in radial feeders with variable short-circuit currents, therefore it is more suitable for feeder protection in vessels. Indeed, operation of OC relays is endangered by variable short-circuit power, as this condition causes variable short-circuit currents, while the ratio between the NSQ and PSQ of the fault current, which is the backbone of the protection system discussed in this paper, does not vary significantly with variation of the short-circuit currents. The proposed method of protection does not require additional hardware or sensors compared to OC relays, so it can be seen as an additional functionality of the existing digital OC relays for improved performance against PP faults.

7. References

[1] Borstlap, R., Ten Katen, H.: 'Ships' electrical systems' (DOKMAR Maritime Publishers BV, 2011, 1st edition)

[2] Van Dokkum, K.: 'Ship knowledge: ship design, construction and operation' (DOKMAR Maritime Publishers BV, 2013, 8th edition), pp. 288-313

[3] Ciontea, C.I., Leth Bak, C., Blaabjerg, F., Madsen, K.K., Sterregaard, C.H.: 'Review of network topologies and protection principles in marine and offshore applications', 25th Australasian Universities Power Engineering Conference, Wollongong, Australia, Sep. 2015

[4] Ciontea, C.I., Leth Bak, C., Blaabjerg, F., Madsen, K.K., Sterregaard, C.H.: 'Decentralized adaptive overcurrent protection for medium voltage maritime power systems', IEEE PES Asia-Pacific Power and Energy Engineering Conference, Xi'an, China, Oct. 2016

[5] Lloyd's Register, 'Rules and regulations for the classification of ships', July 2016

[6] American Bureau of Shipping, 'Rules for building and classing steel vessels', Jan. 2016

[7] Det Norske Veritas - Germanischer Lloyd, 'Rules for classification: ships', Jan. 2017

[8] Hall, D.T.: 'Practical marine electrical knowledge' (Witherby & Co Ltd., 1999, 2nd edition), pp. 25-56

[9] Maes, W.: 'Marine electrical knowledge' (Antwerp Marine Academy, Naval Engineering, 2014), pp. 7-12

[10] Nelson, J.P., Burns, D., Seitz, R., Leoni, A.: 'Grounding of marine power systems: problems and solutions', 51st IEEE Annual Petroleum and Chemical Industry Technical Conference, Basel, Switzerland, 2004, pp. 151-161

[11] Kay, J.A., Arvola, J., Kumpulainen, L., 'Protecting at the speed of light: combining arc flash sensing and are-resistant technologies', IEEE Pulp and Paper Industry Technical Conference, San Antonio, Texas, USA, June 2010

[12] Ciontea, C.I., Leth Bak, C., Blaabjerg, F., Madsen, K.K., Sterregaard, C.H.: 'A feeder protection method against the phase-phase fault using symmetrical components', IEEE Electric Ship Technologies Symposium, Arlington, Virginia, USA, Aug. 2017

[13] Wang, J., Sumner, M., Thomas, D.W.P., Gheertsma, R.D., 'Active fault protection for an AC zonal marine power system', IET Electrical Systems in Transportation, 2011, 1, (4), pp. 156-166

[14] Schuddebeurs, J.D., Booth, C.D., Burt, G.M., McDonald, J.R.: 'Impact of marine power system architectures on IFEP vessel availability and survivability', IEEE Electric Ship Technologies Symposium, Arlington, Virginia, USA, May 2007

[15] Blackburn, J.L.: 'Symmetrical components for power systems engineering' (Marcel Dekker, Inc., 1993), pp. 1-3, pp. 39-45

[16] Kojovic, Lj.A., Witte, J.F.: 'Improved protection systems using symmetrical components', Proc. IEEE PES Transmission and Distribution Conference and Exposition, Atlanta, GA, USA, 2001, vol. 1, pp. 47-52

[17] Rizvi, I.A., Reeser, G.: 'Using symmetrical components for internal external fault discrimination in differential protection schemes', Proc. 66th Annual Conference for Protective Relay Engineers, College Station, TX, USA, Apr. 2013, pp. 68-79

[18] www.deif.com

[19] Ziegler G., 'Numerical distance protection' (Publicis Publishing, Erlangen, 2011)

[20] IEC Std. 60255-151: 'IEC International Standard for Measuring relays and protection equipment – Part 151: Functional requirements for over/under current protection', Edition 1.0, Aug. 2010